EEFECTS OF AN ELECTRIC FIELD ON THE ENERGY RELEASE RATE: A SELF-CONSISTENT ANALYSIS

Tong-Yi Zhang, Cai-Fu Qian and Pin Tong
Department of Mechanical Engineering
Hong Kong University of Science and Technology
Kowloon, Hong Kong

ABSTRACT

The self-consistent method is used to calculate the crack opening profile in a piezoelectric material under combined mechanical and electric loadings. The energy release rate for crack propagation is evaluated using either the un-opened crack profile (before deformation) or opened crack profile (after deformation). The results show that the applied electric field does not influence the energy release rate if the un-opened crack profile is adopted, while the electric field will play an important role when the opened crack profile is used. An analysis on an electrically conductive, elliptical cavity reveals the energy release rate for cavity propagation is a positive definite function of the combined mechanical and electrical loadings.

KEYWORDS

Fracture, Piezoelectric materials, Crack opening, Self-consistent method, Energy release rate.

INTRODUCTION

The mechanical reliability of piezoelectric materials becomes increasingly important as they are used in more and more sophisticated areas. Thus, there has been tremendous interest in studying the fracture behavior and fracture mechanics of those materials (Pohanka *et al.*, 1976; Pohanka *et al.*, 1978; Cherepanov, 1979; Deeg, 1980; Yamamoto *et al.*, 1983; McMeeking, 1989; Mehta and Virkar, 1990; Pak and Herrmann, 1986; Pak, 1990; Sosa and Pak, 1990; Suo *et al.*, 1992; Zhang and Hack, 1992; Suo, 1993; Kumar and Singh, 1996; Lynch, 1996; Zhang and Tong, 1996; Hom *et al.*, 1996; Gao, Zhang and Tong, 1996). An important issue in studying fracture mechanics of piezoelectric materials is electric boundary conditions along the crack faces. There are two approaches commonly used to specify the boundary conditions. One assumes that the normal component of electric displacement along the crack faces equals zero (Pak, 1990). This boundary condition ignores the electric field within the crack. Another treats the crack as being electrically permeable (Mikahailov and Parton, 1990). Sosa (1991, 1992) investigated the mechanical and electrical fields in the vicinity of circular and elliptical holes and used asymptotic expressions for the electromechanical fields in the vicinity of a crack to study the electric fields' effects on crack arrest and crack skewing. Pak and Tobin (1993) found the

ratio of the crack tip electric field to the applied field approaches unity as an elliptical cavity reduces to a slit crack. Dunn (1994) also investigated the effects of crack face boundary conditions on the energy release rate in piezoelectric solids. His results indicate that the impermeable assumption can lead to significant errors regarding the effects of the electric fields on crack propagation based on an energy release rate criterion. In a previous paper (Zhang and Tong, 1996), we studied the boundary conditions by considering an elliptical cylinder cavity. In the limiting process, we found that the two commonly used boundary conditions are actually two extremes of the exact boundary conditions. Since the electric field exists in air and in a vacuum, both the geometry and size of the crack have a great influence on fracture behavior of these materials (Zhang, 1994; Zhang and Tong, 1996). For the case that a crack is treated as a mathematical slit crack without any thickness, the energy release rate for crack propagation evaluated from linear fracture mechanics is positive definite and independent of applied electric fields when the electric field inside the crack is considered (McMeeking, 1989; Zhang and Tong 1996). On the other hand, the energy release rate is not positive definite and the electric loading would always impede crack propagation when the electric field inside the crack is ignored (Pak, 1990; Suo *et al.*, 1992). A mathematical slit crack opens under combined mechanical-electrical loadings and becomes a cavity. Thus, the electric field would have a great influence on the fracture behavior when the opened crack is considered. The self-consistent method is adopted here to determine the crack opening and hence the energy release rate.

The following section reports the profile calculation of a slit crack opening using the self-consistent method. Then, the energy release rate for crack or cavity propagation is evaluated under a condition that the ratio of the minor semi-axis to the major semi-axis of the elliptical profile of the crack opening maintains unchanged. All the derived formulas are confirmed by finite element analysis and plotted to demonstrate explicitly the effects of electric field on the energy release rate and the differences between the present work and others.

ANALYSIS

Self-consistent Calculation for Crack Opening Profile

Considering a mathematical slit crack in an infinite piezoelectric material under combined mechanical and electrical loadings, as shown in Fig. 1, where the crack is perpendicular to the poling direction and applied loadings are applied also in the poling direction, the analytical solutions can be closely formulated from conventional linear elastic analysis via the Stroh formalism (Stroh, 1958). Under a pure mechanical loading, the crack profile either before or after deformation can be used to evaluate the stress fields and the energy release rate as long as the deformation is small. Under combined mechanical and electrical loadings, however, the crack opens and the crack deformation is very sensitive to the electric field inside the opened crack, which, in turn,

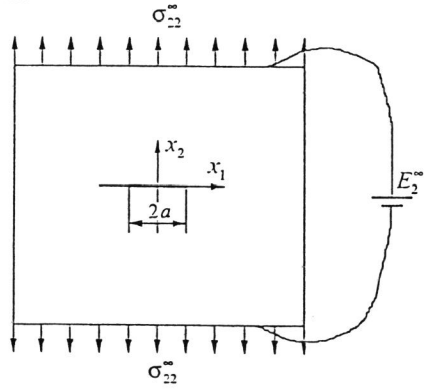

Fig. 1. A slit crack in an infinite piezoelectric medium under combined mechanical and electrical loadings.

is affected by the opened crack profile. A geometrically non-linear analysis, here called self-consistent calculation, is thus adopted to determine the deformed crack profile and subsequently the energy release rate for the crack propagation.

For a slit crack, the crack opening along the x_2 axis, Δu_2 from conventional calculations (i.e., without considering the geometrically non-linear behavior of the crack), is given by

$$\Delta u_2 = a\left[(\mathbf{B}+\overline{\mathbf{B}})(\Sigma_2^a - \mathbf{d})\right]_2 \sin\theta, \quad 0 \le \theta \le \pi, \tag{1}$$

where the superscript 'a' means applied, $2a$ is the crack length, θ is the polar angle, $\mathbf{B}$ is a 4x4 matrix depending on the material properties and crack orientation, and

$$\mathbf{d} = (0,0,0,d)^T, \qquad \Sigma_2 = (\sigma_{12}, \sigma_{22}, \sigma_{32}, D_2)^T, \tag{2}$$

where the superscript "T" denotes the transpose of a matrix, d is a parameter related to the electric field inside the crack and D is the electric displacement. Clearly, the profile of the crack opening is an ellipse with the major semi-axis of a and the minor semi-axis of $b = \frac{a}{2}\left[(\mathbf{B}+\overline{\mathbf{B}})(\Sigma_2^a - \mathbf{d})\right]_2$. Thus, the ratio α_c of the minor semi-axis to the major semi-axis evaluated from conventional calculation is:

$$\alpha_c = \frac{1}{2}\left[(\mathbf{B}+\overline{\mathbf{B}})(\Sigma_2^a - \mathbf{d})\right]_2, \tag{3}$$

which will be compared with the results obtained from the self-consistent calculation later.

The self-consistent method requires that the half maximum opening of the elliptical cylinder cavity should be equal to the minor semi-axis. That means

$$\alpha_s = \left[\mathbf{A}\mathbf{f}(\alpha_s) + \overline{\mathbf{A}\mathbf{f}(\alpha_s)}\right]_2 \quad at\ (0,0), \tag{4}$$

where α_s is the ratio of the minor semi-axis to the major semi-axis in the self-consistent calculation, the overbar denotes the conjugate of a complex, $\mathbf{A}$ is also 4x4 matrix depending on the material properties and crack orientation, and $\mathbf{f}(\alpha_s)$ is a 4-dimensional vector, and a function of α_s and the remote loadings. After tedious algebra calculation, Eq. (4) is finally re-arranged as

$$g_0 + g_1\alpha_s + g_2\alpha_s^2 + g_3\alpha_s^3 = 0, \tag{5}$$

where g_0, g_1, g_2 and g_3 are real parameters related to the material properties, crack orientation, and the loading conditions.

The Energy Release Rate for Crack or Cavity Propagation

The energy release rate can be evaluated from each of the four thermodynamic functions: free energy, electric enthalpy, mechanical enthalpy and full Gibbs energy, or from each of the four associate potentials. In the present work, we follow Rice's treatment (1968) and use the potential associated with the electric enthalpy to formulate the energy release rate. Using the same principal and methodology, we first derive the energy release rate for an elliptical cavity, as shown in Fig. 2, under the condition that a constant ratio of the minor semi-axis to the major semi-axis, $\alpha_s = b/a$ is maintained. When the elliptical cavity reduces to a slit crack, the energy release rate will automatically respond for crack propagation. Since only two-dimensional problems are treated here, all properties are calculated per thickness. For the loading conditions studied in the present work, the energy release rate is given by

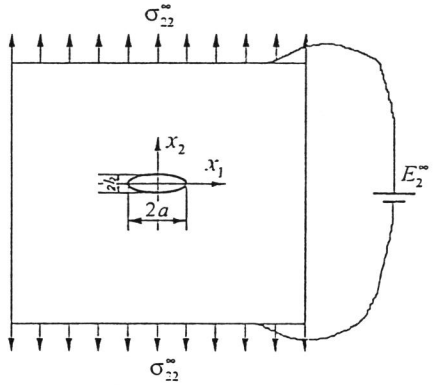

Fig. 2. An elliptical cavity in an infinite piezoelectric medium under combined mechanical and electrical loadings.

$$J = \frac{\pi a}{4}\Big[(\Sigma_2^a)^T(\mathbf{B}+\overline{\mathbf{B}})\Sigma_2^a - (1+\alpha)(\Sigma_2^a)^T(\mathbf{B}\bar{\mathbf{d}}+\overline{\mathbf{B}}\mathbf{d}) - i(1+\alpha)(\bar{\mathbf{d}}-\mathbf{d})^T(\mathbf{A}\mathbf{a}_1+\overline{\mathbf{A}\mathbf{a}_1})$$
$$-\alpha\Big[(1+\alpha)(\bar{\mathbf{d}}+\mathbf{d}) - 2\Sigma_2^a\Big]^T[\mathbf{A}<p_i>\mathbf{a}_1 + \overline{\mathbf{A}}<\overline{p_i}>\overline{\mathbf{a}_1}]\Big\} \qquad (6)$$

where Σ_2^a is a 4-dimensional vector for applied loadings, <> denotes a diagonal matrix, p_i (i=1, 2, 3,4) are the eigen-roots with positive imaginary parts determined by the material properties and crack orientation and $\mathbf{a}_1$ is a 4-dimensional vector depending on the remote loadings. Eq. (6) shows that the energy release rate for elliptical cavity growth depends on both mechanical and electric loads, as well as on the ratio of $\alpha = b/a$ and the electric field inside the cavity.

When the cavity reduces to a slit crack, $\alpha = b/a = 0$ and hence

$$d = \frac{(B+\overline{B})_{4i}\Sigma_{2i}^a}{2B_{44}}. \qquad (7)$$

Thus, the energy release rate can be explicitly expressed in terms of the remote loads as

$$J = \frac{\pi a}{4}\sum_{i,j=1}^{3}\sigma_{i2}^a\left[(B+\overline{B})_{ij} - \frac{(B+\overline{B})_{i4}(B+\overline{B})_{4j}}{2B_{44}}\right]\sigma_{j2}^a. \qquad (8)$$

Eq. (8) shows that the energy release rate relies only on the applied mechanical loads, being independent of the applied electric load. This phenomenon was found before by McMeeking (1989), Zhang and Hack (1992) and Zhang and Tong (1996).

Electric Field in the Cavity and Crack

From the conventional analysis, the electric field in an elliptical cavity or a slit crack can be formulated. Introducing $E = E_1 - iE_2$, where E_1 and E_2 represent the electric field in the x_1 and x_2 directions, respectively, leads to the following form of the electric field inside an elliptical cavity in an infinite piezoelectric medium under combined mechanical and electric loadings:

$$E = -i2(B_4+\overline{\mathbf{B}_4})\frac{m(1+\kappa_c B_{44})\overline{\mathbf{La}_1^*} + (1-\kappa_c B_{44})\mathbf{La}_1^*}{m^2(1+\kappa_c B_{44})^2 - (1-\kappa_c B_{44})^2} \qquad (9)$$

where $m = (a-b)/(a+b)$, $\mathbf{L}$ is also 4x4 matrix depending on the material properties and crack orientation, $\mathbf{a}_1^*$ is a 4-dimensional vector depending on the applied loadings and material properties. It is seen that the electric field within the cavity is uniform.

For a slit crack, the electric field inside the crack is

$$E = -i(B_4+\overline{\mathbf{B}_4})\frac{\Sigma_2^a + \kappa_c B_{44}(\overline{\mathbf{La}_1} - \mathbf{La}_1)}{\kappa_c B_{44}}. \qquad (10)$$

Eq. (10) shows that if the dielectric constant κ_c of the crack has a finite value, the electric field inside the crack is also uniform.

RESULTS AND DISCUSSION

The present work uses the PZT-4 ceramics as a model material. The material constants are given below:

Elastic constants ($10^{10}\ N/m^2$):
$c_{11} = 13.9$, $c_{12} = 7.78$, $c_{13} = 7.43$,
$c_{33} = 11.3$, $c_{44} = 2.56$;
Piezoelectric constants (C/m^2):
$e_{31} = -6.98$, $e_{33} = 13.84$,
$e_{15} = 13.44$;
Dielectric constants ($10^{-9}\ F/m$):
$\kappa_{11} = 6.00$, $\kappa_{33} = 5.47$;
$\kappa_c = 8.85 \times 10^{-3}$;

where N and C denote, respectively, Newton and Coulomb. The dielectric constant of vacuum, κ_c, is also listed here for convenience.

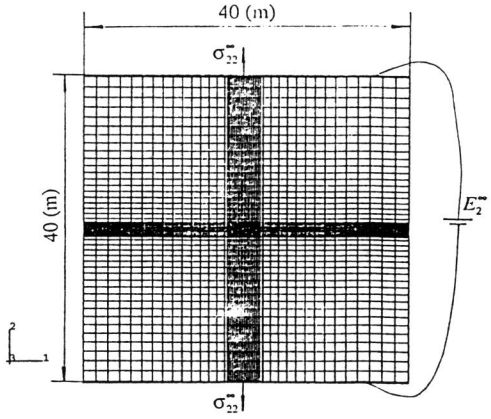

Fig. 3(a). Finite element mesh for a centered elliptical cavity in a large piezoelectric medium under combined mechanical and electrical loadings.

In order to verify the validity of the formulas presented in the previous section, we resort to the finite element analysis and the commercial software ABAQUS is used in the analysis. The example considered is a finite medium with a centered crack or elliptical cavity under both mechanical and electrical loadings. The specimen dimensions, finite element mesh and loading conditions are shown in Fig. 3(a) for the case of a centered elliptical cavity, with Fig. 3(b) being the magnification of the mesh around the cavity. As the medium size is much larger than that of the crack or cavity, the near tip solution should be nearly the same as that for the infinite medium. 8-nodded plain strain elements were used in the analysis.

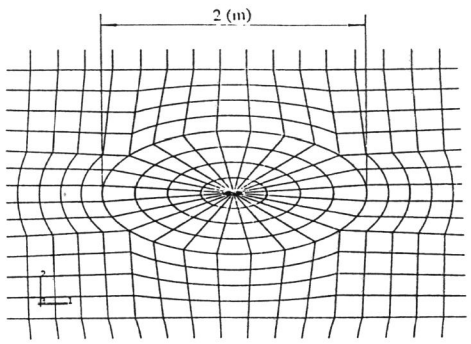

Fig. 3(b). Mesh around the cavity.

Fig. 4 shows the distribution of the stress σ_{22} and electric field strength E_2 in front of the right major axial apex of an elliptical cavity with the major semi-axis $a=1m$ and the minor semi-axis $b=0.2m$ under combined mechanical and electrical loadings in the x_2 direction. As expected, both the stress and the electric fields are concentrated at the apex of the cavity and the analytical results agree well with the finite element analysis, which indicates that the analytical solutions for an elliptical cylinder cavity in a infinite piezoelectric medium under combined mechanical and electric loadings are all valid.

Finite element evaluation of the energy release rate J is based on the following formula:

$$J=\int_{\Gamma}(Hn_1-\sigma_{ij}n_j u_{i,1}+D_i E_1 n_i)d\Gamma, \qquad (11)$$

where

$$H=\frac{1}{2}c_{ijkl}\varepsilon_{ij}\varepsilon_{kl}-\frac{1}{2}\kappa_{ij}E_iE_j-e_{ikl}\varepsilon_{kl}E_i$$ is

the electric enthalpy; Γ is an integration contour around the crack tip or ellipse apex, $\mathbf{n}$ is the unit normal vector to the contour, σ_{ij}, ε_{ij}, u_i, E_i and D_i represent stresses, strains, displacements, electric fields and electric displacements, respectively. For a piezoelectric problem, when the dielectric constant of the medium inside the crack or elliptical cavity is considered non-zero, the electric field inside the cavity makes contributions to the J-integral (i.e., the energy release rate), thus, the integration contour should include the path inside the crack or cavity. The integration contour coincides with the minor semi-axis when across the

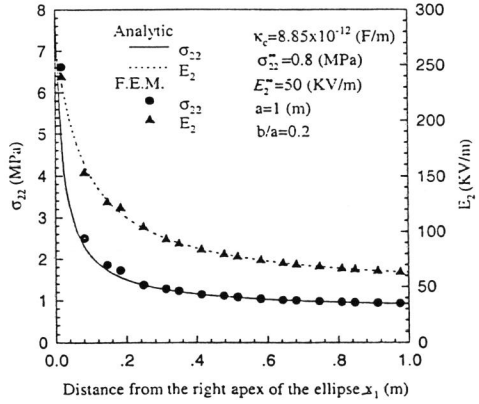

Fig. 4. Distribution of stress σ_{22} and electric field E_2 ahead of an elliptical cavity .

elliptical cavity.

The numerical calculations show that the electric field inside the cavity is uniform, which is consistent with the analytical results indicated by Eq. (9). For a given cavity, both the electric field inside the cavity and the energy release rate for the cavity propagation are functions of the applied mechanical and electric loadings. Fig. 5 shows the variations of the electric field inside the cavity and the energy release rate with the applied stress under a constant applied electric field when the cavity medium is considered as a vacuum. The electric field inside the cavity is about 5 times as high as the applied electric field and increases its absolute magnitude with increasing the applied stress. The energy release rate increases as the absolute value of the applied stress increases. It could hold for an elliptical cavity that the energy release rate increases with increasing absolute value of a compressive-applied stress as long as the upper and lower faces do not contact each other. When the upper and lower faces of the cavity contact, which could be the case for a slit crack under compress, the traction-free condition along the cavity faces does not hold any more, and then the energy release rate loses its meaning. Under a constant applied stress, Fig. 6 shows the electric field inside the cavity and the energy release rate as a function of the applied electric field. The electric field inside the cavity is about 5 times as high as the applied electric field. Either a positive or a negative applied electric field decreases the energy release rate. When the cavity is reduced to a slit crack, the electric field inside the crack is around 1,000 times as high as the applied electric field, as shown in Fig. 7, and the energy release rate becomes independent of the applied electric loading. As shown in Figs. 5, 6 and 7, the theoretical predictions of the energy release rate, i.e., Eqs. (6) and (8) are well confirmed by the finite element analysis. With all formulas being confirmed by finite element analysis, hereafter, we will not have to present the finite element results in the following discussion.

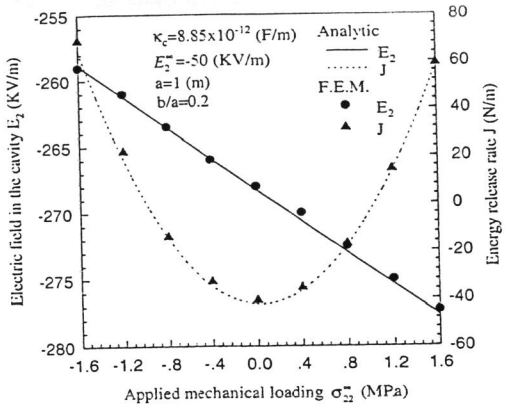

Fig. 5. Electric field and energy release rate as a function of applied mechanical loading for a vacuumed elliptical cavity.

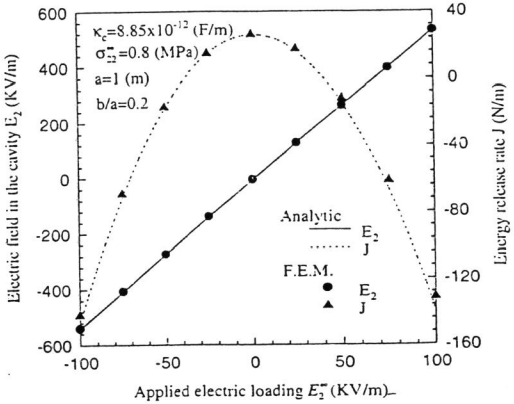

Fig. 6. Electric field and energy release rate as a function of applied electric loading for a vacuumed elliptical cavity.

In Figs. 5 and 6, the medium inside the cavity is considered a vacuum that has the smallest dielectric constant. To demonstrate the influence of the cavity medium, we now consider another extremity, i.e., an infinitely large dielectric constant for the cavity that represents a conducting cavity. Fig. 8 shows the electric field inside the cavity and the energy release rate J as a function of the applied electric loading when the mechanical loading is constant and the dielectric constant of the medium in the cavity is taken as 1,000 times of the outside piezoelectric medium (i.e. κ_c/κ_{33}=1,000). As expected, the electric field inside the cavity is almost zero, but the energy release rate J is positive definite with the change of applied electric loading, which is totally different from that for a vacuumed elliptical cavity as shown in Fig. 6. The energy release rate J is also positive definite with the change of applied mechanical loading as shown in Fig. 9, which also differs from that for a vacuumed elliptical cavity as shown in Fig. 5 in which J could be negative when the mechanical loading is low and the electric loading is high. An electrically-positive-defined energy release rate means that the electric loading would cause the crack propagation rather than impede it.

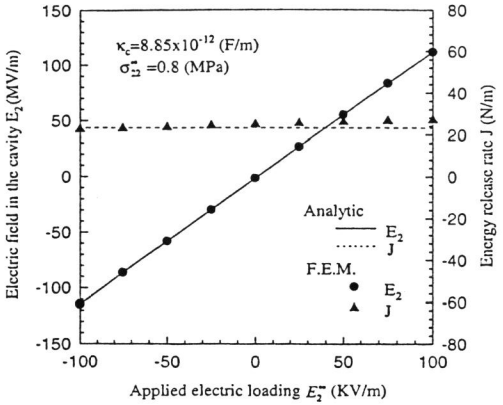

Fig. 7. Electric field and energy release rate vs. applied electrical loading for a vacuumed slit crack.

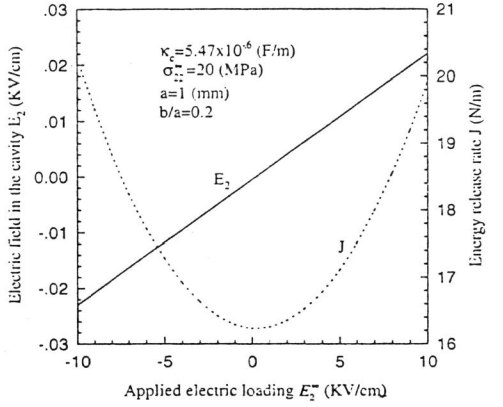

Fig. 8. Electric field and energy release rate as a function of applied electrical loading for an electrically conductive ellipitical cavity.

As argued in the last section and discussed above, since the effect of the applied electric loading on a slit crack is totally different from that on an opened crack, it is more reasonable to determine the final crack surface profile under combined mechanical and electrical loadings by introducing an elliptical crack geometry with a to-be-determined minor semi-axis. Fig. 10 shows α_s evaluated from the self-consistent calculation by Eq. (5), together with α_c for a slit crack obtained from conventional calculation by Eq. (3) as a function of the electric loading when the mechanical loading is constant. It is found that if the electric loading is zero, α_s is equal to α_c and both are proportional to the mechanical loading. If the electric loading is not zero, however, α_s is different from α_c and the difference becomes larger as the magnitude of the electric field increases. It is also found in Fig. 10 that the direction of the electric loading also affects the value of α_s (i.e. the opening of the cavity). Compared with the crack opening without electric loading, a positively applied electric loading makes the crack opening larger while a negatively applied electric loading makes the crack opening smaller.

Since the geometry of a crack also affects its propagation, the deformed crack profile should be used in the calculation of the energy release rate. Fig. 11 shows the energy release rate calculated using the deformed crack profile α_s, as shown in Fig. 10. Since the magnitude of α_s is very small under the loading range, the energy release rate is almost symmetric-about E_2=0 when the crack medium is considered a vacuum, while the energy release rate is about constant for an electrically conducting crack. If the applied electric loading is much larger, the influence of α_s would emerge and the energy release rate would be expected to be asymmetric for a vacuumed crack and inconstant for a conducting crack. Fig. 12 compares the energy release rate obtained from the self-consistent calculation with those from conventional calculations. It is clear that the resistance of the applied electric loading to propagation of a vacuumed crack is overestimated if the electric field inside the crack is ingored, as shown in Fig. 12. In Fig. 13, the deformed crack profile α_s was used and the energy release rate was fixed as the same as that when only mechanical loading was applied, e.g. σ_{22}^{∞}=20 MPa. It is seen that for a vacuumed crack, the applied loading increases with increasing the magnitude of applied electric loading, implying that the applied loading will impede the crack propagation. For a conducting crack, a constant energy release rate leads to to the result that the applied mechanical load is almost independent of the electric load, as shown in Fig. 13.

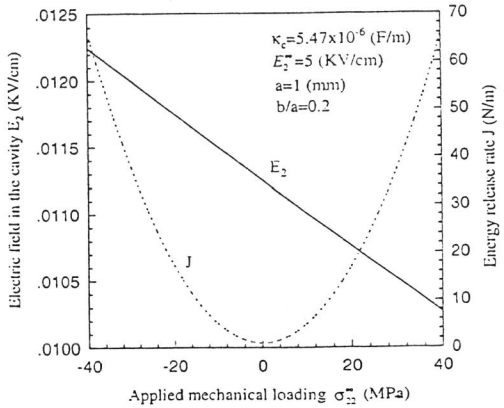

Fig. 9. Electric field and energy release rate as a function of applied mechanical loading for an electrically conductive elliptical cavity.

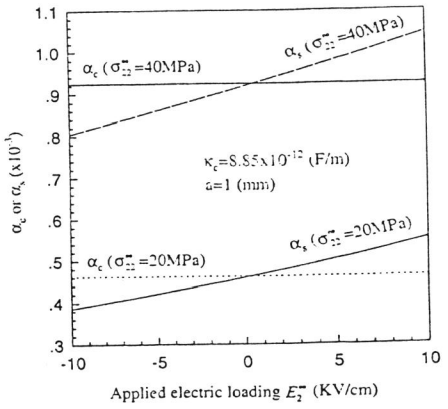

Fig. 10. Comparison of a self-consistent calculation with a conventional calculation for crack deformation under combined mechanical and electrical loadings.

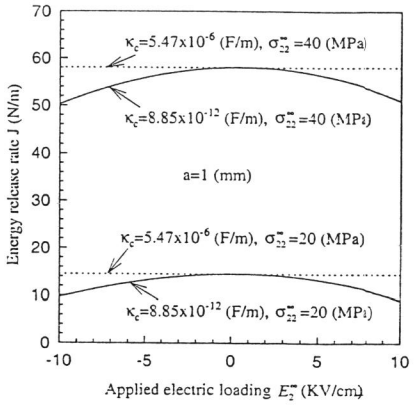

Fig. 11. Energy release rate as a function of applied electrical loading using the crack profile calculated by the self-consistent method.

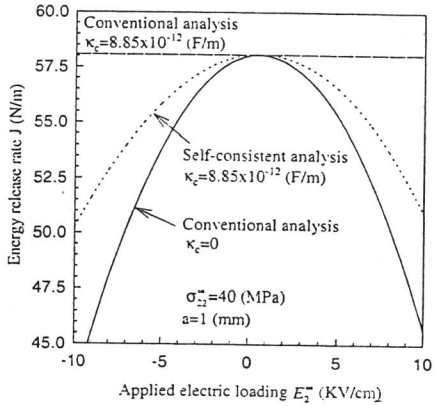

Fig. 12. Comparison of the self-consistent calculation with the conventional one for energy release rate.

CONCLUDING REMARKS

This paper presents a self-consistent calculation for a deformed crack profile in an infinite piezoelectric medium under combined mechanical and electrical loadings. The effects of electrical loadings on the energy release rate for crack or cavity propagation have been studied. The results show that for a slit vacuumed crack, the energy release rate is independent of the applied electric loading while the electrical field inside the crack magnifies the remote electric loading by more than 1,000 times. The energy release rate for propagation of an elliptical cavity with a constant ratio of the minor semi-axis to the major semi-axis is a function of both electrical and mechanical loadings, the ellipse geometry and the dielectric constant of the cavity. For an electrically conductive elliptical cavity, the energy release rate is a positive definite function of the applied electrical and/or mechanical loadings. However, these results

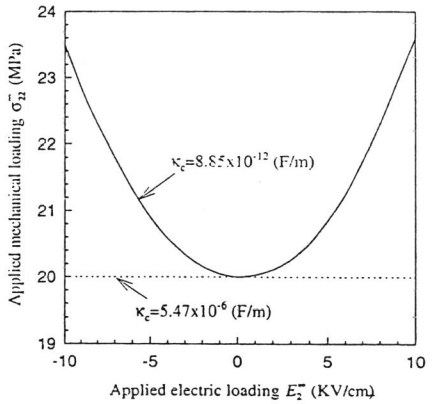

Fig. 13. Applied mechanical loading as a function of applied electrical loading for a given energy release rate.

do not provide a linear relationship between the energy release rate and the applied electric field that was observed in the indentaion tests (Yamamoto, et al., 1983; Tobin and Pak, 1993) and the fracture tests (Park and Sun, 1995). Recently, Gao, Zhang and Tong (1996) proposed, by analogy with the classical Dugdale model, an electric strip saturation model and hence derived the local and global energy release rates. Under small scale yielding conditions, the global energy release rate equals to that of a linear piezoelectric crack without electrical yielding. The local energy release rate gives linear predictions which agrees with above mentioned experimental results.

ACKNOWLEDGMENTS

The authors thank Professor Huajian Gao from Stanford University for useful discussions. Financial support from the Hong Kong Research Grants Council under RGC grant HKUST573/94E is gratefully acknowledged.

REFERENCES

Cherepanov, G.P. (1979) *Mechanics of Brittle Fracture*, McGraw-Hill, New York, pp. 317-341.

Deeg, W.F.J. (1980) The analysis of dislocation, crack, and inclusion problems in piezoelectric solids. *PhD Thesis*, Stanford University.

Dunn, M.L. (1994) The effects of crack face boundary conditions on the fracture mechanics of piezoelectric solids. *Engng. Frac. Mech.* **48,** 25-39.

Gao, H., Zhang, T.Y. and Tong, P. (1996) Local and global energy release rates for an electrically yielded crack in piezoelectric ceramics, submitted to *J. Mech. Phys. Solids.*

Hom, C. L., Brown, S.A. and Shankar, N. (1996) Constitutive and failure models for relaxor ferroelectric ceramics, *in Proceedings of Smart Structures and Materials 1996: Mathematics and Control in Smart Structures*, ed. Varadan, V.V and Chandra, J., **2715,** 316-328.

Kumar, S. and Singh, R.N. (1996) Crack propagation in piezoelectric materials under combined mechanical and electrical loadings, *Acta mater.* **44,** 173-200.

Lynch, C.S. (1996) Residual stress contribution to fracture of ferroelectric ceramics, *in Proceedings of Smart Structures and Materials 1996: Mathematics and Control in Smart Structures*, ed. Varadan, V.V and Chandra, J., **2715,** 359-365.

Makino, H. and Kmiya, N. (1994) Effects of dc electric field on mechanical properties of piezoelectric ceramics. *Jpn. J. Appl. Phys.* **33,** 5323-5327.

McMeeking, R.M. (1989) Electrostrictive stresses near crack-like flaws. *J. Appl. Math. Phys.* **40,** 615-627.

Mehta, K. and Virkar, A.V. (1990) Fracture mechanisms in ferroelectric-ferroelastic lead zirconate titanate (Zr:Ti=0.54:0.46) ceramics. *J. Am. Ceram. Soc.*, **73,** 567-574.

Mikahailov, G.K. and Parton, V.Z. (1990) *Electromagnetoelasticity*. Hemisphere, New York.

Pak, Y.E. (1990) Crack extension force in a piezoelectric material. *J. Appl. Mech.* **57,** 647-653.

Pak, Y.E. and Herrmann, G. (1986) Conservation laws and the material momentum tensor for the elastic dielectric. *Int. J. Engng. Sci.* **24,** 1365-1374.

Pak. Y.E. and Tobin. A. (1993) On electric field effects in fracture of piezoelectric materials. *Mech. Electromagn. Mater. Structures* **AMD 161/MD 42**, 51-62.

Pohanka, R.C., Rice, R.W. and Walker, B.E., Jr. (1976) Effect of internal stress on the strength of $BaTiO_3$. *J. Am. Ceram. Soc.*, **59**, 71-74.

Pohanka, R.C., Freiman, S.W. and Bender, B.A. (1978) Effect of phase transformation on the fracture behaviour of $BaTiO_3$. *J. Am. Ceram. Soc.*, **61**, 72-75.

Rice, J.R. (1968) Mathematical analysis in the mechanics of fracture. *Fracture, Volume II* (ed. H. Liebowitz) pp.191-311, Academic Press, New York.

Sosa, H. and Pak, Y.E. (1990) Three-dimensional eigenfunction analysis of a crack in a piezoelectric material. *Int. J. Solids Structures* **26,** 1-15.

Sosa, H. (1991) Plane problems in piezoelectric media with defects. *Int. J. Solids Structures* **28,** 491-505.

Sosa, H. (1992) On the fracture mechanics of piezoelectric solids. *Int. J. Solids Structures* **29,** 2613-2622.

Stroh, A. N. (1958) Dislocations and cracks in anisotropic elasticity. *Phil. Mag.* **3**, 625-646.

Suo, Z., Kuo, C.M., Barnett, D.M. and Willis, J.R. (1992) Fracture mechanics for piezoelectric ceramics. *J. Mech. Phys. Solids* **40,** 739-765.

Suo, Z. (1993) Models for breakdown-resistant dielectric and ferroelectric ceramics. *J. Mech. Phys. Solids* **41,** 1155-1176.

Tobin. A. and Pak. Y.E. (1993) Effect of electric fields on fracture behavior of PZT ceramics. in *Proceedings of Smart Structures and Materials 1993*, ed. Varadan, V.V, **1916**, 78-86.

Yamamoto, T., Igarashi, H. and Okazaki, K. (1983) Internal stress anisotropies induced by electric field in Lanthanum modified $PbTiO_3$ ceramics. *Ferroelectrics*, **50**, 273-278.

Zhang, T.Y. and Hack, J.E. (1992) Mode-III cracks in piezoelectric materials. *J. Appl. Phys.* **71,** 5865-5870.

Zhang, T.Y. (1994) Effect of sample width on the energy release rate and electric boundary conditions along crack surfaces in piezoelectric materials. *Int. J. Fracture* **66**, R33-R38.

Zhang, T.Y. and Tong, P (1996) Fracture mechanics for a mode-III crack in a piezoelectric material. *Int. J. Solids Structures* **33**, 343-359.